

# In Situ-Formed $\text{Li}_2\text{S}$ in Lithiated Graphite Electrodes for Lithium–Sulfur Batteries

Yongzhu Fu, Chenxi Zu, and Arumugam Manthiram\*

Electrochemical Energy Laboratory &amp; Materials Science and Engineering Program, University of Texas at Austin, Austin, Texas 78712, United States

**S** Supporting Information

**ABSTRACT:** Rechargeable lithium–sulfur (Li–S) batteries have the potential to meet the high-energy demands of the next generation of batteries. However, the lack of lithium in the sulfur cathode requires the use of lithium metal anode, posing safety hazards. Use of  $\text{Li}_2\text{S}$  as the cathode can eliminate this problem, but it is hampered by intrinsic challenges (e.g., high electrical resistivity and reactivity in air). We report here the use of a lithiated graphite electrode to chemically reduce *in situ* the polysulfide  $\text{Li}_2\text{S}_6$  in liquid electrolyte to insoluble  $\text{Li}_2\text{S}$ . The chemical reduction slowly draws lithium out of graphite, resulting in a reduction of the  $d_{002}$  spacing of graphite from 3.56 to 3.37 Å and an increase in the open-circuit voltage of cells from 60 mV to 2.10 V after stabilizing over 6 days. X-ray photoelectron spectroscopic analysis shows 48.4% of sulfur in the polysulfide was converted to  $\text{Li}_2\text{S}$ . The formed amorphous  $\text{Li}_2\text{S}$  shows good cyclability with low charge overpotential. The results demonstrate that lithiated graphite can serve as a lithium donor in lithium-deficient cathodes, which could enable lithium metal-free Li–S, Li–air, or Li–organic batteries.

Lithium-ion (Li-ion) batteries have been successful as power supplies for portable electronics over the last two decades. The high operating voltage and energy density make them unmatched by other aqueous electrolyte-based rechargeable batteries.<sup>1</sup> To further increase the energy density of Li-ion batteries to meet the increasing demand of existing portable electronics markets and the burgeoning needs of electric vehicles and smart grids, alternative high-capacity electrode materials beyond the insertion compound electrodes (e.g., graphite anode and  $\text{LiCoO}_2$  and  $\text{LiMn}_2\text{O}_4$  cathodes) are critically needed, e.g., silicon anode<sup>2</sup> and sulfur and oxygen (air) cathodes.<sup>3</sup> However, the use of these high-capacity electrodes is hampered by unprecedented challenges due to their undesirable intrinsic properties: complex redox reactions involving multiple electrons and significant volume changes accompanying morphology and phase transitions upon cycling.

Sulfur as a cathode material for lithium–sulfur (Li–S) batteries has been studied over 50 years, and the persistent challenges are its low electrical conductivity, dissolution of lithium polysulfides into the liquid electrolyte, and the shuttle effect of these soluble species.<sup>4</sup> Recent efforts, e.g., sulfur–carbon composites,<sup>5–7</sup> core–shell structures,<sup>8–10</sup> and trapping polysulfides within the cathode region,<sup>11,12</sup> have shown

significant performance improvements that are close to practical applications. However, the lack of lithium in the sulfur cathode requires the use of a lithium metal anode, which poses serious safety hazards and may not be practical. Some efforts have recently been focused on the development of lithium sulfide ( $\text{Li}_2\text{S}$ ) cathodes,<sup>13–16</sup> which could lead to lithium metal-free Li–S batteries. The intrinsic properties of  $\text{Li}_2\text{S}$ , e.g., high resistivity and high reactivity in air, make it highly challenging in fabricating practical  $\text{Li}_2\text{S}$  cathodes. For example, direct use of  $\text{Li}_2\text{S}$  powder may require the first charge to high voltages ( $\geq 4$  V) to make  $\text{Li}_2\text{S}$  active due to the large particle size of  $\text{Li}_2\text{S}$ ;<sup>13,16</sup> also, chemical synthesis of  $\text{Li}_2\text{S}$ –carbon composites needs multiple sophisticated steps.<sup>15</sup>

Lithium polysulfides ( $\text{Li}_2\text{S}_n$ ,  $n > 2$ ) are intermediate compounds between elemental sulfur and  $\text{Li}_2\text{S}$ , which can be generated in liquid electrolytes by the reaction  $(n - 1)\text{S} + \text{Li}_2\text{S} \rightarrow \text{Li}_2\text{S}_n$  and used as cathode materials.<sup>17</sup> For example, the polysulfide  $\text{Li}_2\text{S}_6$  can be electrochemically converted to sulfur/high-order polysulfides during charge ( $\text{Li}_2\text{S}_6 \rightarrow 6\text{S} + 2\text{Li}^+ + 2\text{e}^-$ ) or insoluble  $\text{Li}_2\text{S}$  during discharge ( $\text{Li}_2\text{S}_6 + 10\text{Li}^+ + 10\text{e}^- \rightarrow 6\text{Li}_2\text{S}$ ) in a Li/polysulfide cell.<sup>18</sup> On the other hand, lithium can be electrochemically intercalated into graphite to form  $\text{LiC}_6$  and reversibly deintercalated. The lithium stored in the lithiated graphite with a chemical potential close to that of metallic lithium would be a strong reducing agent for chemical reactions, but it has not yet been explored. Herein, we demonstrate that lithiated graphite can donate lithium to chemically reduce  $\text{Li}_2\text{S}_6$  *in situ* in liquid electrolytes to insoluble  $\text{Li}_2\text{S}$ , serving as a starting cathode material in Li/polysulfide cells.

The intercalation/deintercalation of lithium into/from graphite has been well investigated.<sup>19–21</sup> Toray carbon paper (CP) was selected in this study because it contains graphite like in other carbon papers reported.<sup>22</sup> The woven fibers in the carbon paper (Figure S1) not only provide a structural integration during the cell fabrication but also act as a current collector in the electrode. Figure 1A shows the first discharge (lithiation) voltage profile, and Figure S2 shows the continuous voltage profile and stable cyclability of the carbon paper in a half cell with lithium anode. The major voltage profile lies below 0.2 V, corresponding to the multistage formation of lithiated  $\text{Li}_x\text{C}_6$  ( $0 < x \leq 1$ ) as in graphite anodes.<sup>21</sup> The discharged carbon paper has a golden yellow color, which is also an indication of lithium intercalated graphite. The lithiated

Received: October 1, 2013

Published: November 18, 2013

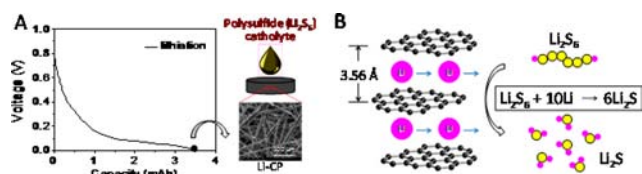


**Figure 1.** (A) First discharge (lithiation) voltage profile of graphitic carbon paper and a schematic showing a drop of dissolved polysulfide  $\text{Li}_2\text{S}_6$  in liquid electrolyte added into the lithiated carbon paper electrode, with the zoomed-in SEM image showing the fibrous structure of the lithiated carbon paper electrode. (B) Schematic showing the chemical reduction reaction of one  $\text{Li}_2\text{S}_6$  molecule by lithium to form six  $\text{Li}_2\text{S}$  molecules, involving the diffusion/driving of lithium out of the graphene layers in the graphite.  $\text{Li}_2\text{S}_6$  represents the average molecular formula of polysulfides in the liquid electrolyte, and 3.56 Å is the spacing of (002) planes in the lithiated graphite in the carbon paper.

carbon paper was then used to fabricate a Li/polysulfide cell with the dissolved polysulfide  $\text{Li}_2\text{S}_6$  electrolyte added into the cathode side. The large voids in the carbon paper, as seen in the SEM images in Figure 1A and Figure S1, can accommodate the polysulfide electrolyte introduced.

The potential of  $\text{Li}_2\text{S}_6$  is  $\sim 2.28$  V vs  $\text{Li}/\text{Li}^+$  in the liquid electrolyte used,<sup>18</sup> whereas that of the lithiated carbon paper is close to 0.01 V vs  $\text{Li}/\text{Li}^+$  after the first discharge. The huge potential difference ( $>2.2$  V) between them results in a spontaneous chemical reduction of  $\text{Li}_2\text{S}_6$  when they are in contact with each other, involving the diffusion/consumption of lithium out of lithiated graphite, as depicted in Figure 1B. The capacity of lithium during the first discharge of the carbon paper used is  $\sim 3.4$  mAh, which is higher than the theoretical capacity (3.2 mAh) of the polysulfide  $\text{Li}_2\text{S}_6$  used [for details, see the Supporting Information], providing enough lithium to convert all the  $\text{Li}_2\text{S}_6$  to  $\text{Li}_2\text{S}$ .

Figure 2A shows the XRD pattern of the pristine CP, lithiated carbon paper (Li-CP), and the Li-CP with polysulfide after a prolonged stabilizing time ( $\geq 6$  days) (designated as  $\text{Li}_2\text{S-CP}$ ). The CP shows a strong peak at  $27.2^\circ$  and a weak peak at  $55.2^\circ$ , corresponding, respectively, to the (002) and (004) reflections of graphite.<sup>23</sup> After lithiation, the (002) reflection shifts to a lower angle of  $24.9^\circ$ , indicating an increase in the interplanar spacing  $d_{002}$  from 3.28 to 3.56 Å due to the intercalation of lithium ions into the graphite layers. The reflection is, however, split due to the inhomogeneous distribution of lithium inside the graphitic layers of the carbon paper. The reduction of  $\text{Li}_2\text{S}_6$  by Li-CP involves extraction of lithium from Li-CP, resulting in a shifting of the (002) reflection to  $26.6^\circ$  in  $\text{Li}_2\text{S-CP}$  and a compacting of the interplanar spacing  $d_{002}$  to 3.35 Å. The (004) reflection also undergoes a similar transition process. A detailed evolution of the XRD patterns as a function of stabilizing time (1–6 days) is shown in Figure S3 and the corresponding changes in the  $d_{002}$  spacings are listed in Table S1. The structural evolution of graphite in the Li-CP electrode used with  $\text{Li}_2\text{S}_6$  is similar to that in the electrochemical delithiation of Li-CP, as compared in the XRD patterns in Figure S3. The reflections broaden, and the peak intensity decreases in  $\text{Li}_2\text{S-CP}$ , implying a decrease in the long-range order of the graphitic planes and destructive interferences caused by the reduced products on the surface of graphite.<sup>24</sup> There are no additional identifiable crystalline peaks, indicating that the formed sulfur-containing species are largely in amorphous state.

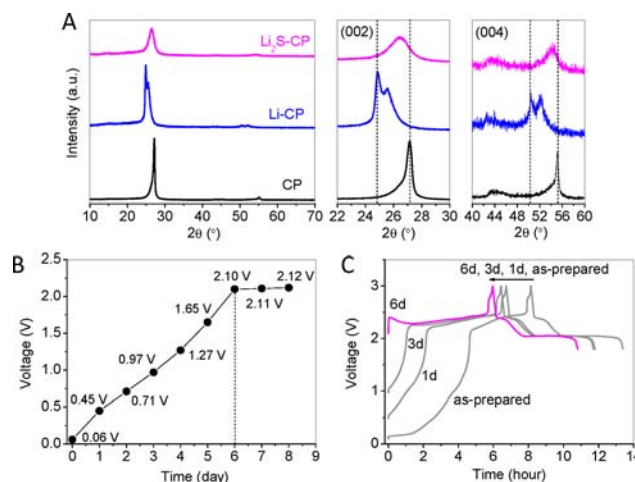


**Figure 2.** (A) XRD patterns of the pristine CP, Li-CP, and the Li-CP with polysulfide after a prolonged stabilizing time ( $\geq 6$  days) (designated as  $\text{Li}_2\text{S-CP}$ ), with the two zoomed-in XRD patterns on the right showing the region of the (002) reflection at  $2\theta = 22^\circ\text{--}30^\circ$  and the region of the (004) reflection at  $2\theta = 40^\circ\text{--}60^\circ$ . (B) OCV of a Li/polysulfide cell with a Li-CP electrode as a function of stabilizing time (day). (C) Voltage profile of the first charge and discharge of Li/polysulfide cells before (as-prepared) and after 1 day (1d), 3 day (3d), and 6 day (6d) stabilizing.

The as-prepared Li/polysulfide cell with the Li-CP- $\text{Li}_2\text{S}_6$  cathode and lithium metal anode has an open circuit voltage (OCV) of  $\sim 60$  mV, which almost linearly increases to 2.10 V over 6 days and then stabilizes at 2.12 V, as shown in Figure 2B. The slow reaction between  $\text{Li}_2\text{S}_6$  and lithium in Li-CP is partially due to the low diffusivity of lithium in Li-CP<sup>25</sup> and the blocking of lithium diffusion out of Li-CP by the reduced products formed on the surface of Li-CP. Figure 2C shows the voltage profile of the first charge and discharge of the Li/polysulfide cells after various stabilizing times. The as-prepared cell shows a voltage plateau below 0.2 V at the beginning of charge followed by a slow increase to 2 V. Above 2 V, a low charge voltage plateau appears which is not seen in the first charge of the control Li/polysulfide cell with a pristine CP electrode as displayed in Figure S4. This charging process indicates that some lithium is still in the graphite (Li-CP), and some have reacted with  $\text{Li}_2\text{S}_6$  to form reduced sulfur compounds which have a higher voltage. After 1 and 3 day stabilizing, the charge voltage plateau below 2 V obviously shortens. At the same time, the low charge voltage plateau above 2 V elongates and the voltage increases. After 6 days stabilizing, the OCV increases to 2.10 V, and there is no charge voltage plateau below 2 V anymore. With only a small overpotential in the first charge supported by the amorphous reduced products formed, the charge process shows two overlapping charge voltage plateaus which are characteristic of the electrochemical oxidation of  $\text{Li}_2\text{S}$ .<sup>18</sup> After the first charge, all the cells show a characteristic discharge voltage profile (two distinct discharge voltage plateaus at  $\sim 2.3$  and 2.1 V) of Li-S batteries, which resemble that of the control Li/polysulfide cell shown in Figure S4. Cyclic voltammogram (CV) shown in Figure S5 and the voltage profile shown in Figure S6 of the cells further confirm the  $\text{Li}_2\text{S}$ -like behavior of the  $\text{Li}_2\text{S-CP}$  electrode which contains a small amount of partially reduced sulfur species.

The charge and discharge capacities of the cells shown in Figure 2C along with the Coulombic efficiency in the first cycle

are listed in Table 1. The charge capacity starts at 2.61 mAh and then decreases to 1.91 mAh after 6 day stabilizing, which

**Table 1. Charge and Discharge Capacities and Coulombic Efficiency in the First Cycles of Li/Polysulfide Cells with Li-CP Electrodes after Different Stabilizing Time  $t$**

$t$ (day)	first charge capacity (mAh)	first discharge capacity (mAh)	Coulombic efficiency (%)
0	2.61	1.64	62.8
1	2.16	1.55	71.8
3	2.07	1.67	80.7
6	1.91	1.51	79.1

are all higher than the discharge capacities, but lower than the initial capacity (i.e., 3.4 mAh) of the Li-CP electrode. The loss of the initial charge capacity could be due to the irreversible side reactions, e.g., reduction of  $\text{LiNO}_3$  additive occurring at  $<1.6\text{ V}$ ,<sup>26</sup> which could consume lithium. The Coulombic efficiency is 62.8% initially and finally stabilizes at  $\sim 80\%$ . Without  $\text{LiNO}_3$  additive in the electrolyte, the stabilizing time shortens to 4 days, and the final OCV still stabilizes at 2.12 V, but the first charge cannot be completed and the first discharge does not exhibit the high voltage plateau at 2.3 V as shown in Figure S7, which are due to the shuttle effect.<sup>27</sup>

To further prove this concept, alternative catholytes with higher concentration (0.5 M  $\text{Li}_2\text{S}_6$ ) and other solvents (e.g., tetraglyme and sulfolane without  $\text{LiNO}_3$ ) were investigated. The OCV as a function of time and first cycle voltage profile are shown in Figure S8. With higher concentration polysulfide, the OCV of the cell stabilizes at around 2.1 V after only 4 days, and the cell shows a similar charge and discharge voltage profile as that in Figure 2C but without the initial overpotential after stabilizing. However, the OCVs of the cells with tetraglyme or sulfolane slightly increase to 80–90 mV over 6 days indicating both solvents are not favorable for the *in situ* chemical reduction of  $\text{Li}_2\text{S}_6$  to form  $\text{Li}_2\text{S}$ . The long first charge voltage profile implies minimum side reactions that consume lithium in the Li-CP electrode, which confirms the side reaction discussed above is mostly due to the chemical reduction reaction of  $\text{LiNO}_3$  in the electrolyte.

In addition, a Li/polysulfide cell with a conventional lithiated graphite (MCMB) electrode was also evaluated. The OCV of the cell follows an increasing and then stabilized trend as those of the cells with the Li-CP electrodes, and the cell with 0.5 M  $\text{Li}_2\text{S}_6$  after stabilizing can be charged and discharged, showing the electrochemical behavior of  $\text{Li}_2\text{S}$ , as shown in Figure S9. These results confirm that  $\text{Li}_2\text{S}$  can be formed *in situ* with conventional lithiated graphite.

To identify the  $\text{Li}_2\text{S}$  formed, the  $\text{Li}_2\text{S}$ -CP electrodes before and after the first cycle (charge and discharge) were analyzed by XPS. Figure 3A presents the S  $2p_{3/2}$  and S  $2p_{1/2}$  dual peaks with an intensity ratio of  $\sim 2:1$  arising from spin orbit coupling. The lone dual peaks at high binding energies (172–167 eV) are the characteristic of S in  $\text{LiCF}_3\text{SO}_3$ .<sup>18</sup> There are three pairs of S  $2p_{3/2}$  and S  $2p_{1/2}$  dual peaks in the low binding energy region (165–158 eV) in both the electrodes. The S  $2p_{3/2}$  peaks centered at 163.2, 161.7, and 160.1 eV can be assigned to S in  $\text{Li}_2\text{S}_x$  ( $x < 6$ ),  $\text{Li}_2\text{S}_2$ , and  $\text{Li}_2\text{S}$ , respectively.  $\text{Li}_2\text{S}_x$  and  $\text{Li}_2\text{S}_2$  are both partially reduced compounds of  $\text{Li}_2\text{S}_6$ . Their contents are listed in Table 2. About 48.4% of  $\text{Li}_2\text{S}_6$  is converted to  $\text{Li}_2\text{S}$  in the chemical reduction and 54.9% in the electrochemical reduction. The incomplete chemical reduction reaction in the

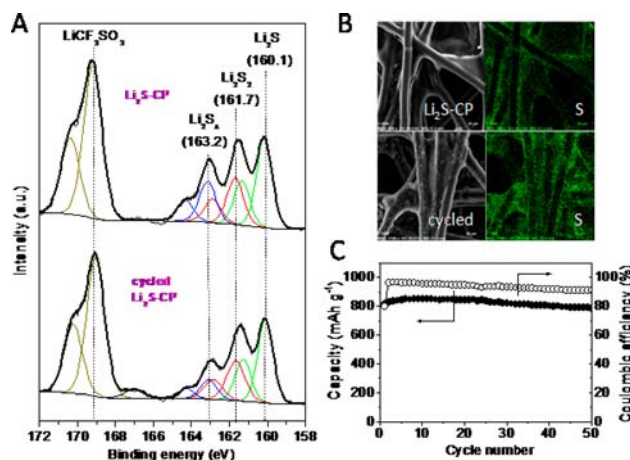


**Figure 3.** (A) Sulfur (S) 2p XPS spectra of the  $\text{Li}_2\text{S}$ -CP electrode before and after the first cycle (charge and discharge). (B) SEM images and S mapping of the  $\text{Li}_2\text{S}$ -CP electrode before and after the first cycle. (C) Discharge capacity and Coulombic efficiency of a half cell with the  $\text{Li}_2\text{S}$ -CP electrode at a rate of C/10 ( $1\text{C} = 1672\text{ mA g}^{-1}$  of sulfur); the capacities are based on the mass (1.9 mg) of sulfur in the polysulfide  $\text{Li}_2\text{S}_6$  used in the half cell.

**Table 2. Compositions of Reduced Sulfur Compounds in the  $\text{Li}_2\text{S}$ -CP Electrode before and After the First Cycle (charge and discharge) Based on the XPS Analysis Shown in Figure 3A**

sample	$\text{Li}_2\text{S}$ (%)	$\text{Li}_2\text{S}_2$ (%)	$\text{Li}_2\text{S}_x$ (%)
	(160.1 eV)	(161.7 eV)	(163.2 eV)
$\text{Li}_2\text{S}$ -CP	48.4	26.9	24.7
cycled $\text{Li}_2\text{S}$ -CP	54.9	30.5	14.6

$\text{Li}_2\text{S}$ -CP electrode is because of the insoluble  $\text{Li}_2\text{S}$  and  $\text{Li}_2\text{S}_2$  formed on the surface of graphite blocking the pathway for the reduction reaction. The  $\text{Li}_2\text{S}_x$  is partially soluble, as indicated by the XPS analysis on the washed electrodes shown in Figure S10 and Table S2. The similar compositions in the  $\text{Li}_2\text{S}$ -CP and its cycled electrode indicate that lithiated graphite can chemically reduce polysulfides to a chemical state that is achieved by the electrochemical reduction in the Li/polysulfide system. The similar XRD patterns (Figure S11) of the two electrodes mean the carbon paper in the  $\text{Li}_2\text{S}$ -CP electrode does not contribute any lithium in the following electrochemical reactions, but only acts as a current collector.

The morphology of the two electrodes is revealed by SEM and sulfur mapping as shown in Figure 3B. The sulfur mapping of the  $\text{Li}_2\text{S}$ -CP indicates that the reduced sulfur compounds are distributed everywhere except the surface of carbon fibers, implying graphite is mostly located in the spaces between fibers. The SEM images and sulfur mapping of the surface and cross-section of the  $\text{Li}_2\text{S}$ -CP electrode shown in Figure S12 indicate a uniform distribution of the formed sulfur compounds. In the cycled electrode, the reduced sulfur compounds are deposited on both the carbon fibers and spaces between them. Figure 3C shows the cyclability of the half cell with a stable discharge capacity of  $\sim 800\text{ mAh g}^{-1}$  over 50 cycles. The Coulombic efficiency starts at  $\sim 80\%$  in the first cycle, increases to over 90% in the second cycle, and then stabilizes. The capacity obtained is largely determined by the structure of the electrode.<sup>28</sup> The large voids in the carbon paper electrodes seen in Figure 3B are not an ideal environment for the electrochemical reactions of



Li<sub>2</sub>S cathodes. With smart designed graphite and electrode structures, the utilization of sulfur can be further improved. Additional cycling performances of the Li<sub>2</sub>S-CP electrode at various rates (e.g., C/5, C/2, and 1C) are shown in Figure S13.

In summary, this study, for the first time, shows the utilization of lithium in lithiated graphite to chemically reduce *in situ* the polysulfide Li<sub>2</sub>S<sub>6</sub> in liquid electrolyte to insoluble Li<sub>2</sub>S as a cathode material for rechargeable Li–S batteries. This chemical reduction reaction process is evident from the distinct interplanar spacing changes in graphite, evolution of the electrochemical behavior of the electrode, and compositional analysis of the reduced sulfur compounds in the electrode. The formed Li<sub>2</sub>S shows low overpotential in the first charge and good cyclability. This approach offers a new way to introduce lithium into the cathode in Li–S batteries and potentially become applicable for other lithium-free or lithium-deficient electrode materials, e.g., oxygen and organic cathode materials. Moreover, the lithiated graphite could be a lithium source for organic synthesis reactions.

## ■ ASSOCIATED CONTENT

### 📄 Supporting Information

Experimental details and materials characterization. This material is available free of charge via the Internet at <http://pubs.acs.org>.

## ■ AUTHOR INFORMATION

### Corresponding Author

manth@austin.utexas.edu

### Notes

The authors declare no competing financial interest.

## ■ ACKNOWLEDGMENTS

This work was supported by the U.S. Department of Energy, Office of Basic Energy Sciences, Division of Materials Sciences and Engineering under award number DE-SC0005397.

## ■ REFERENCES

- (1) Goodenough, J. B.; Kim, Y. *Chem. Mater.* **2010**, *22*, 587.
- (2) Chan, C. K.; Peng, H.; Liu, G.; McIlwrath, K.; Zhang, X. F.; Huggins, R. A.; Cui, Y. *Nat. Nanotechnol.* **2008**, *3*, 31.
- (3) Bruce, P. G.; Freunberger, S. A.; Hardwick, L. J.; Tarascon, J.-M. *Nat. Mater.* **2012**, *11*, 19.
- (4) Ji, X.; Nazar, L. F. *J. Mater. Chem.* **2011**, *20*, 9821.
- (5) Ji, X.; Lee, K. T.; Nazar, L. F. *Nat. Mater.* **2009**, *8*, 500.
- (6) Liang, C.; Dudney, N. J.; Howe, J. Y. *Chem. Mater.* **2009**, *21*, 4724.
- (7) Xin, S.; Gu, L.; Zhao, N.-H.; Yin, Y.-X.; Zhou, L.-J.; Guo, Y.-G.; Wan, L.-J. *J. Am. Chem. Soc.* **2012**, *134*, 18510.
- (8) Jayaprakash, N.; Shen, J.; Moganty, S. S.; Corona, A.; Archer, L. A. *Angew. Chem., Int. Ed.* **2011**, *50*, 5904.
- (9) Seh, Z. W.; Li, W.; Cha, J. J.; Zheng, G.; Yang, Y.; McDowell, M. T.; Hsu, P.-C.; Cui, Y. *Nat. Commun.* **2013**, *4*, 1331.
- (10) Li, W.; Zheng, G.; Yang, Y.; Seh, Z. W.; Liu, N.; Cui, Y. *Proc. Natl. Acad. Sci. U.S.A.* **2013**, *110*, 7148.
- (11) Ji, X.; Evers, S.; Black, R.; Nazar, L. F. *Nat. Commun.* **2011**, *2*, 325.
- (12) Su, Y.-S.; Manthiram, A. *Chem. Commun.* **2012**, *48*, 8817.
- (13) Yang, Y.; Zheng, G. Y.; Misra, S.; Nelson, J.; Toney, M. F.; Cui, Y. *J. Am. Chem. Soc.* **2012**, *134*, 15387.
- (14) Nagao, M.; Hayashi, A.; Tatsumisago, M. *J. Mater. Chem.* **2012**, *22*, 10015.
- (15) Guo, J.; Yang, Z.; Yu, Y.; Abruna, H. D.; Archer, L. A. *J. Am. Chem. Soc.* **2013**, *135*, 763.

(16) Fu, Y.-Z.; Su, Y.-S.; Manthiram, A. *Adv. Energy Mater.* **2013**, DOI: 10.1002/aenm.201300655.

(17) Rauh, R. D.; Abraham, K. M.; Pearson, G. F.; Surprenant, J. K.; Brummer, S. B. *J. Electrochem. Soc.* **1979**, *126*, S23.

(18) Fu, Y.-Z.; Su, Y.-S.; Manthiram, A. *Angew. Chem., Int. Ed.* **2013**, *52*, 6930.

(19) Fong, R.; Sacken, U.; Dahn, J. R. *J. Electrochem. Soc.* **1990**, *137*, 2009.

(20) Dahn, J. R.; Zheng, T.; Liu, Y.; Xue, J. S. *Science* **1995**, *270*, 590.

(21) Jiang, Z.; Alamgir, M.; Abraham, K. M. *J. Electrochem. Soc.* **1995**, *142*, 333.

(22) Snyder, J. F.; Wong, E. L.; Hubbard, C. W. *J. Electrochem. Soc.* **2009**, *156*, A215.

(23) Howe, J. Y.; Rawn, C. J.; Jones, L. E.; Ow, H. *Powder Diffr.* **2003**, *18*, 150.

(24) Stevens, D. A.; Dahn, J. R. *J. Electrochem. Soc.* **2001**, *148*, A803.

(25) Persson, K.; Sethuraman, V. A.; Hardwick, L. J.; Hinuma, Y.; Meng, Y. S.; Ven, A. v. d.; Srinivasan, V.; Kostecki, R.; Ceder, G. *J. Phys. Chem. Lett.* **2010**, *1*, 1176.

(26) Zhang, S. S. *Electrochim. Acta* **2012**, *70*, 344.

(27) Mikhaylik, Y. V.; Akridge, J. R. *J. Electrochem. Soc.* **2004**, *151*, A1969.

(28) Zu, C.-X.; Fu, Y.-Z.; Manthiram, A. *J. Mater. Chem. A* **2013**, *1*, 10362.